JOURNAL OF GEOPHYSICAL RESEARCH, VOL. 95, NO. D4, PAGES 3549-3564, MARCH 20, 1990

Column Atmospheric Water Vapor and Vegetation Liquid Water Retrievals From Airborne Imaging Spectrometer Data

BO-CAI GAO AND ALEXANDER F. H. GOETZ

Center for the Study of Earth from Space/Cooperative Institute for Research in Environmental Sciences, University of Colorado, Boulder

High spatial resolution column atmospheric water vapor amounts were derived from spectral data collected by the airborne visible-infrared imaging spectrometer (AVIRIS), which covers the spectral region from 0.4 to 2.5 μm in 10-nm bands and has a ground instantaneous field of view of 20x20 m from an altitude of 20 km. The quantitative derivation is made by curve fitting observed spectra with calculated spectra in the 1.14-μm and 0.94-μm water vapor band absorption regions using an atmospheric model, a narrow-band spectral model, and a nonlinear least squares fitting technique. The derivation makes use of the facts that (1) the reflectances of many ground targets vary approximately linearly with wavelength in the 0.94- and 1.14-μm water vapor band absorption regions, (2) the scattered radiation near 1 μm is small compared with the directly reflected radiation when the atmospheric aerosol concentrations are low, and (3) the scattered radiation in the lower part of the atmosphere is subjected to the water vapor absorption. The technique is directly applicable for retrieving column water vapor amounts from AVIRIS spectra measured on clear days with visibilities 20 km or greater. The precision of the retrieved column water vapor amounts from several data sets is 5% or better. Based on the analyses of an AVIRIS data set that was acquired within an hour of radiosonde launch, it appears that the accuracy approaches the precision. The derived column water vapor amounts are independent of the absolute surface reflectances. It now appears feasible to derive high spatial resolution column water vapor amounts over land areas from satellite altitude with the proposed high resolution imaging spectrometer (HIRIS). Curve fitting of spectra near 1 μm from areas covered with vegetation, using an atmospheric model and a simplified vegetation reflectance model, indicates that both the amount of atmospheric water vapor and the moisture content of vegetation can be retrieved simultaneously because the band centers of liquid water in vegetation and the atmospheric water vapor are offset by approximately 0.05 μm.

1. INTRODUCTION

Atmospheric water vapor profiles have important applications in many fields, such as meteorology, climatology, infrared astronomy, very long baseline interferometry and high precision geodesy using the global positioning system. High spatial resolution, column water vapor amount can improve the accuracy of satellite humidity sounding [*Susskind et al.*, 1984], be used in micrometeorological studies, in studying the rate of energy exchange between the Earth's surface and the atmosphere and in self-calibration of imaging spectrometer radiance measurements. For the purpose of clarity in this paper, the integrated water vapor content from ground to space in a vertical path is defined as the column water vapor amount in units of centimeters, i.e., the precipitable water vapor.

We have developed a method for quantitative retrievals of high spatial resolution column atmospheric water vapor, which is largely contained in the lower portion of the troposphere, from spectra obtained from the airborne visible-infrared imaging spectrometer (AVIRIS) [*Vane*, 1987] over land areas on clear days with visibilities of 20 km or greater. The method consists of curve fitting observed spectra with simulated spectra in the 1.14-μm (ϕ) or the 0.94-μm (σ) water vapor band absorption region.

In the emerging field of imaging spectrometry of the Earth, great emphasis is being placed on precise knowledge of atmospheric transmission and scattering in order to obtain accurate surface spectral reflectance data from spaceborne measurements [*Goetz et al.*, 1987]. The water vapor values derived from the 1.14- or 0.94-μm band in AVIRIS spectra can be used to remove the effects of other water vapor absorption bands in the 0.4- to 2.5-μm region. Therefore ground level measurements of water vapor amounts simultaneous with AVIRIS and the future high resolution imaging spectrometer (HIRIS) [*Goetz and Herring*, 1989] observations may not be needed for removing water vapor absorption features from the observed spectra.

2. REMOTE SENSING OF ATMOSPHERIC WATER VAPOR

Remote measurement of column water vapor in the atmosphere can be made looking up from the surface or looking down from orbit. Optical methods use the Sun as a source, while microwave and IR methods observe atmospheric emission.

Column water vapor amount can be obtained from the

Paper number 89JD02729.
0148-0227/90/89JD-02729$05.00

ground with a Sun photometer [*Volz*, 1974], or a microwave water vapor radiometer [*Hogg et al.*, 1983]. A Sun photometer measures direct, transmitted solar radiation on clear days in two narrow wavelength regions; one at the center of an absorption band (the 0.94-μm band or the 1.14-μm band) and the other in a "window" just outside the absorption band. A microwave water vapor radiometer measures atmospheric water vapor emission features near 22.2 GHz and works both on clear and cloudy days.

Atmospheric water vapor profiles and column amounts can also be obtained from orbit by measurement of atmospheric emission in the 6- to 12-μm infrared region or near 22.2 GHz in the microwave region. Examples are the HIRS2 (high resolution infrared sounder) and MSU (microwave sounding unit) on board TIROS-N [*Susskind et al.*, 1984]. Experience has shown that above the 500-mbar level, water vapor profiles derived from IR emission spectra are in good agreement with radiosonde data. However, below the 500-mbar level, water vapor profiles derived from IR emission spectra have large uncertainties because of the contributions to the observed radiance from the surface and because of the insensitivity of that radiance to changes in humidity [*Reuter et al.*, 1988]. The HIRS2 column water vapor measurement accuracies over land are only ±25% [*Reuter et al.*, 1988].

Column water vapor amounts over the oceans can be determined with an accuracy of the order of 10% from microwave emission measurements [*Prabhakara et al.*, 1982]. However, it is not possible to derive accurate column water vapor amounts over land from microwave emission measurements because of the highly variable microwave emissivities of land surfaces.

The optical technique described in this paper utilizes the solar radiation reflected by the surface to determine total water vapor amount in the combined path from the Sun to the surface to the sensor. The advantage of the technique over humidity sounding by infrared emission measurements is that the retrieved column water vapor amounts over land surfaces have significantly higher precision. This new technique will complement HIRS2/MSU profiling to yield more accurate measurement of water vapor in the lower troposphere over land.

3. IMAGING SPECTROMETRY

Imaging spectrometers are being developed for remote sensing of the land and coastal waters [*Goetz et al.*, 1985]. Imaging spectrometers acquire images in hundreds of contiguous spectral bands for direct identification of minerals from their characteristic band absorption features [*Hunt and Ashley*, 1979], for studying vegetation biochemistry [*Wessman et al.*, 1988] and water turbidity components [*Gordon and Morel*, 1983]. In the mid 1990s, NASA expects to carry two imaging spectrometers, the moderate resolution imaging spectrometer [*Esias et al.*, 1986] and the high resolution imaging spectrometer (HIRIS) [*Goetz et al.*, 1987] aboard the Earth observing system (Eos) polar platform [*Butler et al.*, 1987]. The precursor to HIRIS, now under development, is the airborne visible-infrared imaging spectrometer (AVIRIS) [*Vane*, 1987]. This instrument images the Earth's surface in 224 spectral bands approximately 10 nm wide, covering the region 0.4-2.5 μm, from an ER-2 aircraft at an altitude of 20 km; the ground instantaneous field of view (GIFOV) is 20x20 m. This field of view will be referred to as a pixel. Four grating-type spectrometers are used to cover the whole range between 0.4 and 2.5 μm. Complete descriptions of the AVIRIS instrument, including radiometric calibration and data processing, are given by *Vane* [1987]. Figure 1*a* shows a diagram of the observational geometry of the AVIRIS instrument. Figure 1*b* shows an example of an AVIRIS spectrum. The absorption features of σ, ϕ, ψ and Ω water vapor bands centered, respectively, at approximately 0.94, 1.14, 1.38 and 1.88 μm are clearly visible. These water vapor features provide the opportunity for derivation of high spatial resolution column water vapor from AVIRIS spectra.

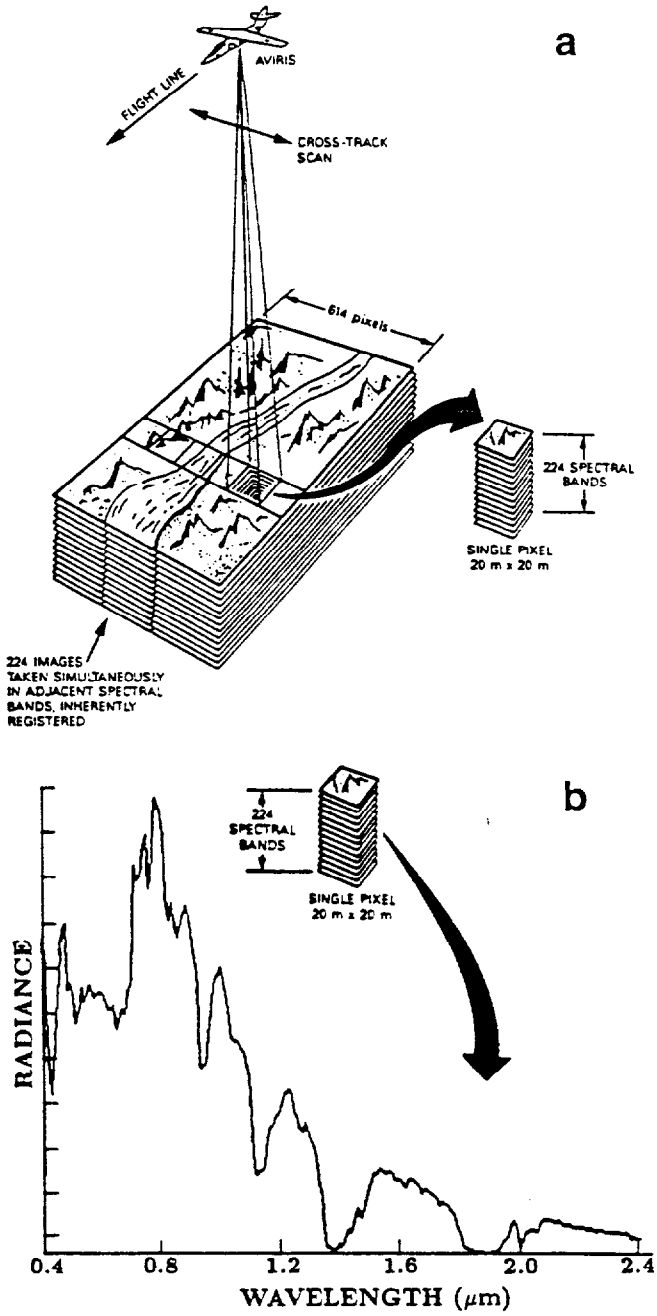

Fig. 1. (*a*) AVIRIS data collection and (*b*) a spectrum from single pixel [from *Vane*, 1987].

4. PRINCIPLES FOR RETRIEVAL OF COLUMN WATER VAPOR AND MOISTURE CONTENT OF VEGETATION FROM AVIRIS SPECTRA

According to *Esaias et al.* (1986), in simplified form, the radiance at a downward looking aircraft sensor can be written as

$$L_{Sensor}(\lambda) = L_{Sun}(\lambda)T(\lambda)R(\lambda) + L_{Path}(\lambda) \quad (1)$$

where λ is the wavelength, $L_{Sensor}(\lambda)$ is the radiance at the imaging spectrometer, $L_{Sun}(\lambda)$ is the solar radiance above the atmosphere, $T(\lambda)$ is the total atmospheric transmittance, which is equal to the product of the atmospheric transmittance from the Sun to the Earth's surface and that from the surface to the aircraft, $R(\lambda)$ is the surface reflectance at the observational geometry, and $L_{Path}(\lambda)$ is the path scattered radiance, including effects of single scattering and multiple scattering. All these, in particular the surface reflectance and the path radiance, must be taken into account in order to derive the atmospheric water vapor amount.

4.1. *The Selection of Water Vapor Bands*

In order to derive the column water vapor with high precision from a water vapor absorption band in a measured spectrum, the transmittances of the band must be sensitive to the change in the number of water vapor molecules in the line of sight. The monthly means of column water vapor in different parts of the United States typically range between 0.5 and 4.3 cm [*Iqbal*, 1983]. Figure 2 shows calculated atmospheric water vapor transmittance spectra between 0.6 and 2.8 μm for water vapor amounts of 0.63, 1.3, 2.5 and 5.0 cm in the line of sight. These transmittance spectra have a spectral resolution of approximately 20 nm. The spectra were calculated with an atmospheric model, the "Tropical Model" from LOWTRAN 6 [*Kneizys*, 1983] and by using a spectral band model described below. These curves indicate that, for the typical atmospheric conditions the transmittances in the 0.94- and 1.14-μm band regions are sensitive to the changes in the amount of water vapor, while in the 1.38- and 1.88-μm band regions they are relatively insensitive to the changes in water vapor amount. The other bands centered at about 0.72, 0.82 and 2.18 μm are too weak to allow accurate retrieval of column water vapor from measured spectra.

Based on these analyses, it is concluded that the 0.94- and the 1.14-μm bands are most useful in column water vapor retrieval from AVIRIS spectra. For simplicity, in this paper only the 1.14-μm water vapor band was used for most of the retrievals.

Figure 2 also shows that under typical atmospheric conditions the water vapor transmittances (not including continuum absorptions) in narrow spectral regions near 0.86, 1.04 and 1.24 μm are greater than 99%. These regions are often referred to as "atmospheric windows."

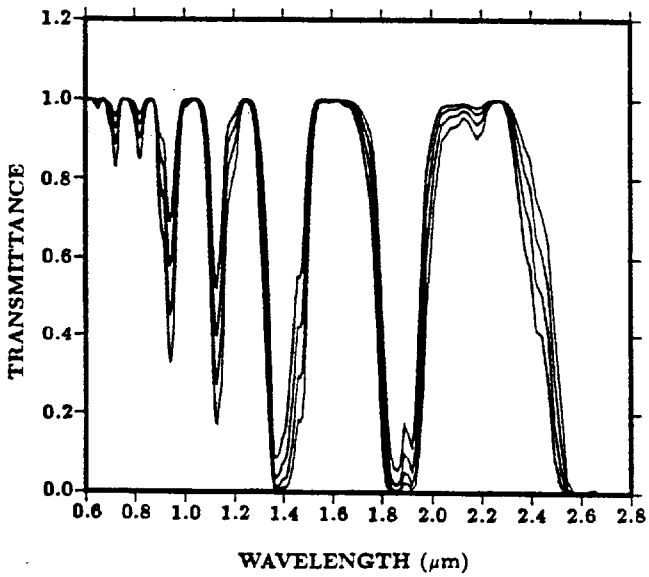

Fig. 2. Vertical atmospheric transmittance as a function of wavelength at different water vapor amounts. The four curves from the top to the bottom correspond to column water vapor amounts of 0.63, 1.3, 2.5 and 5.0 cm, respectively. The calculations were made by using the spectral model described in section 4.2 and the Tropical Model of LOWTRAN6 [*Kneizys et al.*, 1983].

4.2. *A Band Model for Atmospheric Gaseous Absorption*

In order to derive column water vapor amounts from AVIRIS spectra, it is necessary to compare calculated atmospheric spectra with observed spectra. The calculation requires both spectral and atmospheric models.

Each AVIRIS image contains approximately 250,000 spectra, necessitating a fast algorithm for efficient data analysis. A narrow-band spectral absorption model approach is most appropriate for this purpose. The two most commonly used narrow-band (or random-band) models are those of *Goody* [1952] and *Malkmus* [1967]. The Malkmus model is used in our spectral calculations because it allows a more appropriate treatment of intensities of weak lines within a narrow spectral interval [*Malkmus*, 1967]. Letting $T_{\Delta\omega}$ denote the transmittance for a given spectral interval $\Delta\omega$, the Malkmus model is given by

$$T_{\Delta\omega} = \exp\left(-\frac{\pi\Gamma}{2\Delta\omega}\left(\left(1+\frac{4S_{\Delta\omega}m}{\pi\Gamma}\right)^{1/2}-1\right)\right) \quad (2)$$

where $S_{\Delta\omega}$ is the sum of the line intensities within the interval $\Delta\omega$, m is the absorber amount, and Γ is defined by the relation

$$\Gamma = \frac{4}{\pi}\frac{\Sigma\left(S_{JK}\gamma_{JK}\right)^{1/2}}{\Sigma S_{JK}} \quad (3)$$

where S_{JK} and γ_{JK} denote the individual line intensities and line half widths, respectively, and the summation is over all lines within $\Delta\omega$. The band parameters $S_{\Delta\omega}$ and Γ are calculated from the spectral line parameters compiled by

Rothman et al. [1987]. An extension of the Curtis-Godson scaling approximation [*Rodgers and Walshaw*, 1966] is used to take account of the pressure and temperature variations along a typical atmospheric path. Because water vapor continuum absorptions near 1 μm are very weak, these absorptions are not included in our calculations.

In order to gain confidence in the technique, spectra calculated with our program were compared with spectra calculated with a line-by-line program [*Mankin*, 1979] for different observational geometries and with the same atmospheric models. An example of such comparisons is given in Figure 3, which shows a spectrum calculated with our program and a spectrum calculated with the line-by-line program and degraded to a resolution of approximately 20 cm^{-1}. As can be seen, very good agreement was obtained between spectra calculated with both programs. The 20-cm^{-1} spectral resolution, which is higher than the spectra in Figures 1*b* and 2 near 1 μm, allows the small differences in spectra calculated with both programs to be observed. Wave number (cm^{-1}) units are used in Figure 3 instead of wavelength units because most papers on model comparisons present spectra in wave number units.

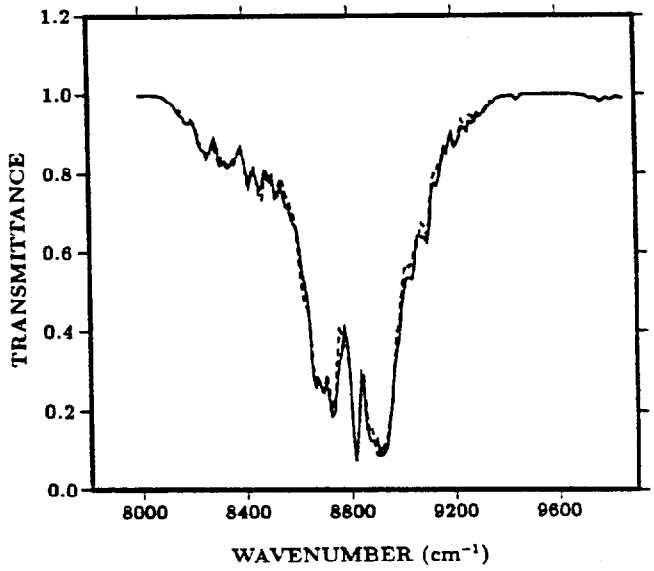

Fig. 3. An example of comparisons of spectra calculated with the narrow-band model (dashed curve) and with a line-by-line program (solid curve) of *Mankin* [1979].

4.3. *The Reflectances of Soils, Rocks, and Vegetation*

Analogous to the aforementioned problems of emittance variability in retrieval of column water vapor over land from HIRS2/MSU, it might be expected that similar difficulties might arise when retrieving column water vapor from AVIRIS spectra because of the variability of reflectances of ground targets. Most of the land areas are covered by soils, rocks, and vegetation. In order to derive water vapor amounts from reflectance spectra over land areas, the reflectance properties of surface targets must be known.

Figure 4 [*Condit*, 1970; *Stoner and Baumgardner*, 1980] shows reflectance curves of typical soils. These reflectance

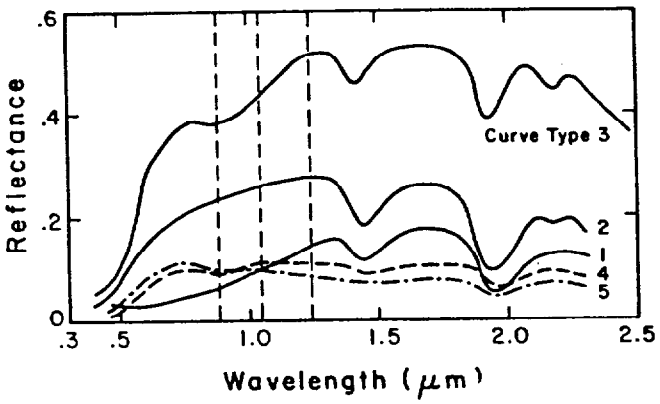

Fig. 4. Typical soil reflectance curves for five major soil types [*Condit*, 1970; *Stoner and Baumgartner*, 1980]: (1) organic-dominated, moderately fine texture; (2) organic-affected, moderately course texture; (3) iron dominated laterite-type soil; (4,5) iron- and organic-rich soil, respectively. The vertical dashed lines represent the 0.94- and 1.14-μm water vapor band regions used in the retrievals.

curves have the common characteristic that the reflectances vary nearly linearly with wavelength in the 0.94-μm and the 1.14-μm water vapor band absorption regions. Similar linearity is observed in reflectances of rocks and minerals, except those of iron-rich minerals.

Soil and rock spectral reflectances in the 0.9- to 1.2-μm region generally increase monotonically except when the iron mineral hematite is present. The Fe^{3+} electronic transition in hematite creates a broad absorption band centered at 0.86 μm, the effects of which extend from 0.75-1.0 μm. The region 0.88-1.05 μm used in water vapor retrievals is located in the longward half of the absorption feature. In the case of retrievals over iron-dominated soils, the departure from the assumed linearity in spectral reflectance over the water vapor band is approximately 4%. This causes an overestimate in retrieved column water of approximately 10%. No other electronic or vibrational absorption features in common rocks or soils produce a significant departure in the linearity of spectral reflectance in the 0.9- to 1.2-μm region.

Surface reflectances of many natural targets in the visible and near infrared regions have been compiled by *Bowker et al.* [1985] from various reported measurements. We selected 74 spectra from the compilation for determining the linearities in the 0.94-μm water vapor band absorption region. The mean of the deviations from linear reflectances is 0.9%, which corresponds to a column water vapor standard deviation of approximately 2.5%.

The linearity allows the quantitative derivations of column water vapor values from AVIRIS spectra over soils and rocks, as discussed below. The reflectance spectrum of vegetation exhibits weak liquid water absorption features centered at approximately 1 and 1.2 μm. The centers of the liquid water bands are shifted by about 0.05 μm to longer wavelengths of the corresponding water vapor band centers. The shifts in wavelength of the bands are due to the larger intermolecular forces of the water molecules in liquid phase than that in the gas phase [*Bunting and d'Entremont*, 1982]. These shifts allow the simultaneous retrievals of column atmospheric water vapor amounts and the moisture

contents of vegetation from AVIRIS spectra over vegetated areas, as described below. Because most wet soils do not have liquid water absorption features at 1 and 1.2 μm [*Bowker et al.*, 1985; J. Margolis, private communication, 1988], the derivation of moisture contents of vegetation from the 1- and 1.2-μm liquid water absorption features is not directly affected by the moisture contents of substrate soils.

4.4. *Column Water Vapor Retrievals From AVIRIS Spectra Over Nonvegetated Areas, Ignoring Scattering*

If atmospheric scattering near 1 μm is neglected, the column water vapor amount over a nonvegetated area can be derived according to the principles described below. The effects of scattering are discussed in section 4.7.

The solid curve in top plot of Figure 5 shows a portion of an AVIRIS spectrum measured over the Cuprite mining district, Nevada, ratioed against a solar radiance curve above the atmosphere. The resulting spectrum is referred to as the "ratioed spectrum." Neglecting scattering and based on the discussions in sections 4.2 and 4.3, we may assume the 1.04- and 1.24-μm regions correspond to the 100% atmospheric gaseous transmission levels. We may also assume that the surface spectral reflectances change linearly with wavelength between these two window regions or equivalently, we may assume that the 100% transmission levels between these two windows can be joined with a straight line. These assumptions permit column water vapor amounts to be retrieved from AVIRIS data without absolute surface reflectances and radiances. Only a relative band-to-band calibration of AVIRIS data over the wavelength region used is required. Curve fitting the ratioed spectrum with a simulated atmospheric gaseous transmission spectrum with appropriate atmospheric and spectral models yields the quantitative amount of water vapor in the line of sight. Spectral curve fitting techniques have been used extensively in quantitative derivation of information on atmospheric trace gases from solar absorption spectra [*Goldman et al.*, 1983; *Farmer et al.*, 1987; *Rinsland et al.*, 1985; *Russell et al.*, 1988; *Shaw et al.*, 1985].

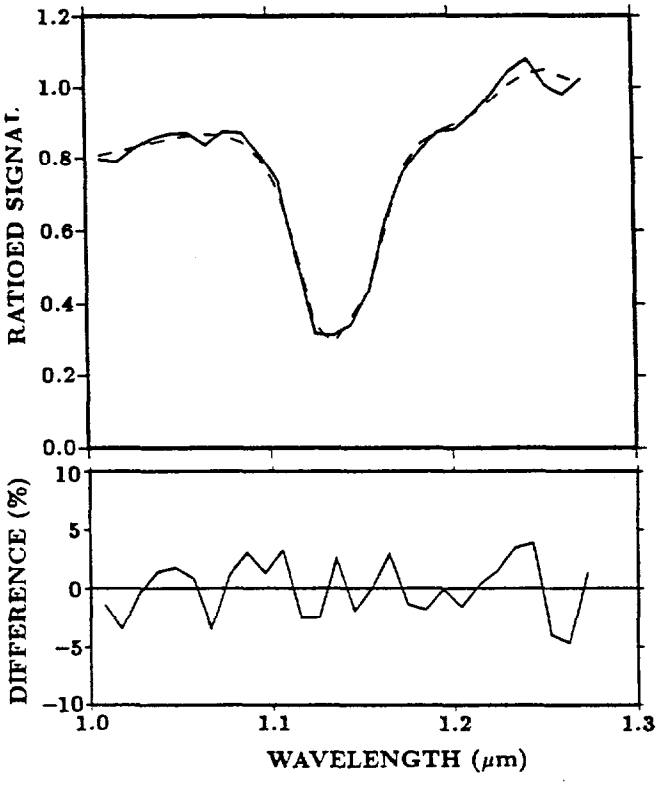

Fig. 5. An example of curve fitting of spectra measured over rocks. The top plot shows the observed spectrum (solid curve) and the fitted spectrum (dashed curve). The bottom plot shows the percent differences between the observed and the fitted spectra.

The dashed curve in top plot of Figure 5 shows the best fit to the ratioed spectrum. The residuals (observed − calculated) expressed as a percentage of the 100% transmission levels are shown in the bottom plot of Figure 5. These residuals have an rms of approximately 5%. The good agreement between the ratioed and the fitted spectra indicates that the Malkmus narrow-band model is adequate for modeling the AVIRIS spectra.

4.5. *Liquid Water Absorption in Vegetation*

The reflection of radiation by vegetation canopies is a complicated absorption and multiple scattering process [*Knipling*, 1970; *Grant*, 1987]. It is controlled by many factors, including (1) the spectral properties of individual leaves, (2) the leaf geometries of vegetation canopies [*Verstraete*, 1988], and (3) the spectral properties of the substrate. Although there has been a considerable amount of theoretical work done to understand and to predict the reflectance of plant canopies [e.g., *Camillo*, 1987; *Dickinson*, 1983; *Dickinson et al.*, 1987; *Otterman*, 1984; *Verstraete*, 1988], there are no models for calculating actual canopy reflectance spectra as a function of wavelength (M. Verstraete, private communication, 1988).

However, the absorption by vegetation between about 0.8 and 3.0 μm is dominated by liquid water attenuation [*Grant*, 1987]. *Allen et al.* [1969] have concluded that a sheet of liquid water can completely account for the absorption spectrum of a single leaf in the 1.4- to 2.5-μm spectral range and the term "equivalent water thickness" (EWT) is used to describe the spectral reflectances of individual leaves between 1.4 and 2.5 μm [*Tucker*, 1980; *Allen et al.*, 1971]. We therefore assume, to a first-order approximation, that the weak water absorption features between 0.9 and 1.3 μm in a reflectance spectrum of vegetation canopy can be described by the transmittances of an equivalent amount of liquid water. The calculation of liquid water transmittances is made by using the liquid water absorption coefficients compiled by *Palmer and Williams* [1974].

4.6. *Column Water Vapor and Equivalent Liquid Water Thickness Retrievals From AVIRIS Spectra Over Vegetated Areas, Ignoring Scattering*

Figure 6 shows calculated transmittances of water vapor, liquid water and ice between 0.6 and 2.8 μm. The ice transmittances were calculated by using the ice absorption coefficients compiled by *Warren* [1984]. The shifts in band centers of water vapor, liquid water and ice are clearly seen

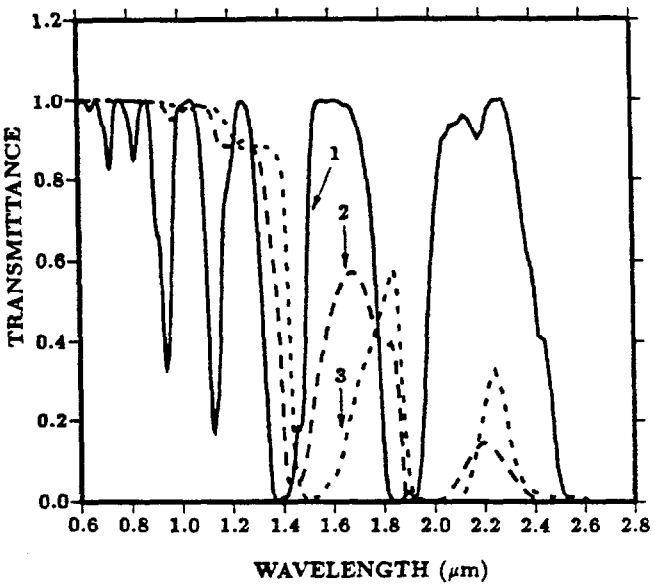

Fig. 6. Calculated transmittances of atmospheric water vapor, liquid water and ice between 0.6 and 2.8 μm. The atmospheric spectrum (curve 1) corresponds to a 5-cm column amount, the liquid water spectrum (curve 2) corresponds to a thickness of 0.1 cm, and the ice spectrum (curve 3) corresponds to a thickness of 0.1 cm. The band centers of water vapor, liquid water and ice are shifted relatively by approximately 50 nm.

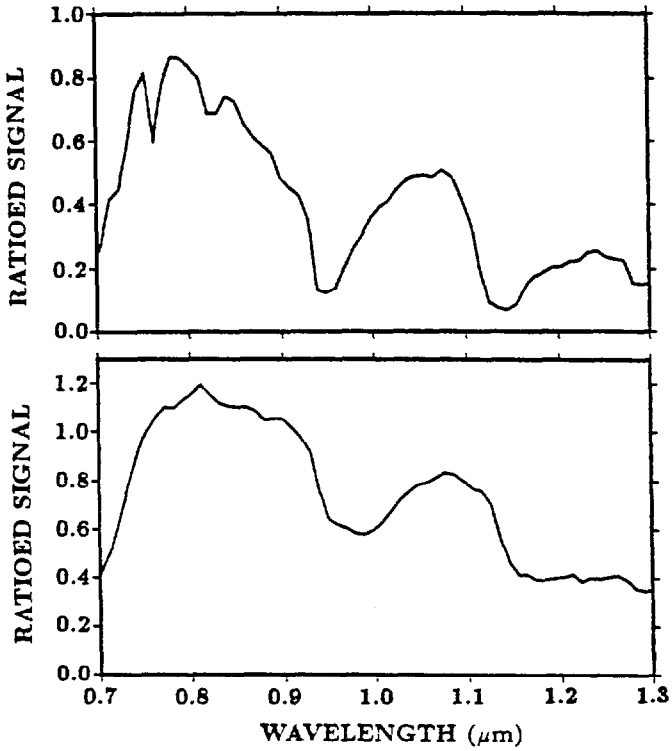

Fig. 7. (Top) An AVIRIS spectrum over vegetation divided by a solar spectrum above the atmosphere, and (bottom) the same AVIRIS spectrum over vegetation divided by a spectrum over an airport runway. The two features centered approximately at 1.0 and 1.2 μm in the bottom plot are the absorption features of liquid water in vegetation. The feature near 0.7 μm is resulted from chlorophyll absorption.

in the figure. The top plot of Figure 7 shows an example of AVIRIS radiances over vegetation divided by solar radiances above the atmosphere. The liquid water absorption features are not discernable in the spectrum dominated by the 0.94- and 1.14-μm atmospheric water vapor bands. The bottom plot of Figure 7 shows the radiances over the same vegetated area but divided by the radiances from a nearby airport runway having nearly constant reflectance around 1 μm. The liquid water absorption features near 1 and 1.2 μm are clearly observed in this plot.

By modeling the shape of the vegetation spectra with the atmospheric band model and the liquid water absorption model described above, both the water vapor amount and the equivalent liquid water thickness can be derived.

4.7. *Scattering*

Typically, atmospheric aerosols are mostly concentrated in the lower 1-2 km of the atmosphere, as are the water vapor molecules. Near 1 μm, the Rayleigh scattering is negligible and the main contribution to the path radiance is the scattering of radiation by aerosols through single and multiple scattering processes. When the aerosol concentration is small (visibilities of 20 km or greater), the single scattering process dominates [*Kneizys et al.*, 1983] and the path radiance near 1 μm is typically of the order of 10% of the direct reflected solar radiation [*Justice and Paris*, 1984; *Iqbal*, 1983]. AVIRIS spectra over water areas and spectra calculated with LOWTRAN7 were used in our studies of path radiance effects, as described below.

Figure 8*a* shows AVIRIS spectra measured over Moffett Field and over a nearby water area in San Francisco Bay. In the 1.04-μm atmospheric window region, the radiance from the water area is about 15% of that from the airport runway. The measured spectrum from the water area also shows the 0.94- and 1.14-μm atmospheric water vapor bands. The radiation near 1 μm over water did not result from any radiation emerging from beneath the water surface, because any solar radiation at this wavelength is completely absorbed [*Kirk*, 1988], but rather from atmospheric scattering. Since the solar zenith angle was 15°, sun glint may also have contributed to the observed radiances. The water vapor absorption features in spectra from the water areas are partly attributed to aerosol scattering along with water vapor absorption within the lower few kilometers of the troposphere. The spectra above 1.27 μm in Figure 8*a* were not reliable because when the measurements were made the spectrometer covering that region was unstable.

Figure 8*b* shows the water and the runway spectra from Figure 8*a* but normalized in the 1.04-μm window region. The 1.14-μm water vapor band absorptions in the two curves are similar. Therefore to a first-order approximation, the path scattered radiation near 1 μm can be treated as a fraction of direct reflected radiation. This means that when the aerosol concentration is small, column water vapor and equivalent liquid water thickness can still be obtained with the simple absorption models described above.

The single scattered radiation reaching the AVIRIS sensor certainly contains shallower water vapor absorption

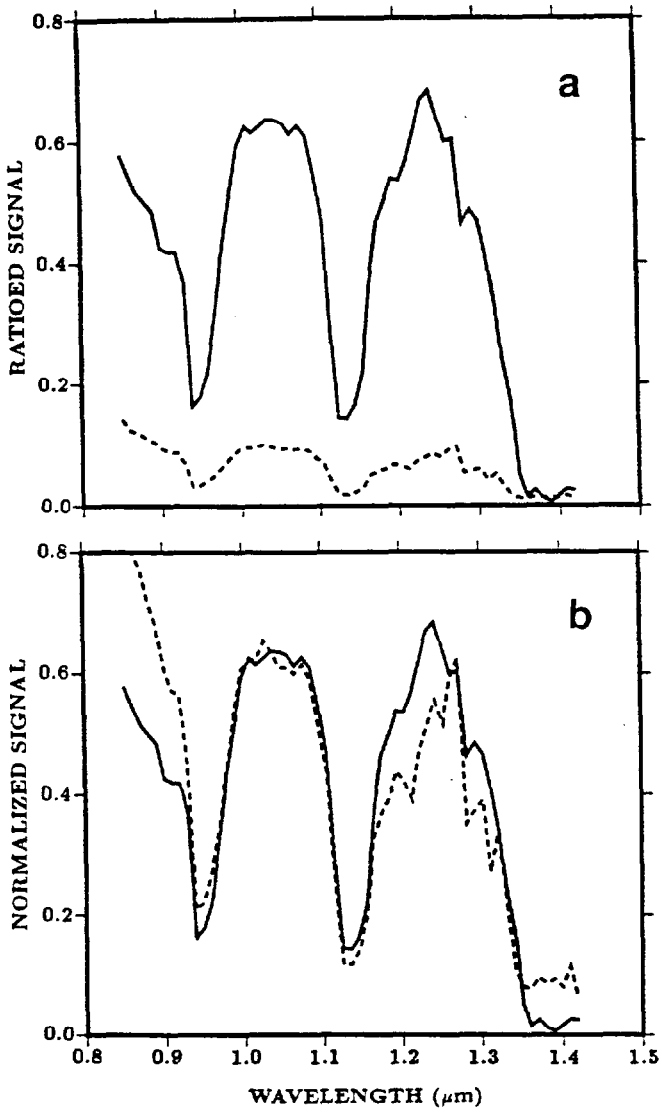

Fig. 8. (*a*) Examples of ratioed spectra over the runway (solid curve) and the water surface (dashed curve), (*b*) Examples of normalized spectra over the runway (solid curve) and the water surface (dashed curve).

features than the direct reflected radiation from the surface because of the shorter ray paths through the atmosphere. Single scattering will therefore lead to an underestimate of column water vapor values with our simple atmospheric transmission model. In order to quantitatively study this effect, spectra were calculated with LOWTRAN7 in the single scattering mode, for the AVIRIS observational geometry, and with surface reflectances between 0.2 and 0.4. Calculations were made without aerosols and with the rural aerosol model having a 23-km visibility. The calculated spectra were then used as the input "observed" spectra in our retrieval program (see section 4.8). The average of retrieved water vapor values from spectra with aerosols is 3.3% less than that without aerosols. Therefore when the aerosol concentrations are low, the single scattering will cause an underestimate of column water vapor values by less than 4% with our retrieving program. Because there is less direct reflected solar radiation over low reflectance areas than over high reflectance areas, the low reflectance areas will be affected more by the single scattering.

The multiple scattered radiation reaching the AVIRIS sensor can act very differently from the single scattered radiation. It can contain deeper water vapor absorption features than the directly reflected radiation because of the longer ray paths in the lower part of the atmosphere. Therefore an offsetting effect in the water vapor absorption features can exist between single and multiple scattered radiation.

4.8. *Retrieval Process*

The procedures for column water vapor retrievals from an AVIRIS spectrum over a nonvegetated area are as follows:

1. The AVIRIS radiance spectrum is divided by the solar radiance curve above the atmosphere. The resulting spectrum is referred to as the "ratioed spectrum."
2. The atmospheric gaseous transmittance, $T(\lambda)$, in the 1.14-μm water vapor band absorption region is calculated with the assumed atmospheric and spectral models.
3. $T(\lambda)$ is multiplied by an initial linear function and then convolved with an instrumental spectral response function (ISRF). The linear function takes account of the linear surface reflectance and the aerosol extinction. The ISRF is assumed to be a Gaussian function with full width at half maximum of 20 nm. The ISRF can also be varied to obtain the least error in the final fit.
4. The calculated spectrum is compared with the ratioed spectrum.

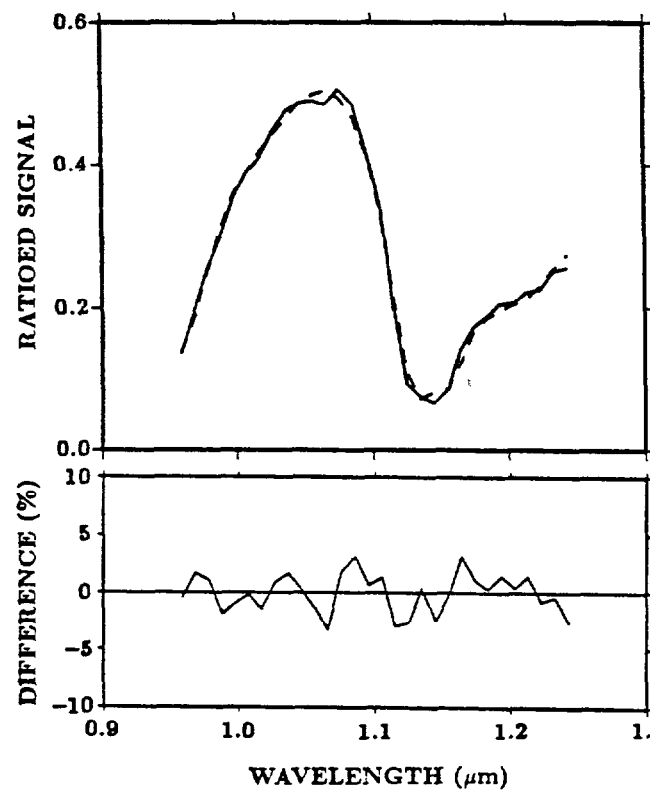

Fig. 9. An example of curve fittings of spectra measured over vegetated areas. The top plot shows the observed spectrum (solid curve) and the fitted spectrum (dashed curve). The bottom plot shows the percent differences between the observed and the fitted spectra.

TABLE 1. The Geographical Information of Relevant AVIRIS Flight Scenes and the AVIRIS Flight Time Over the Scenes

Site	Latitude (N)	Longitude (W)	Date	UT	Comment
Cuprite, Nevada	37°45′	117°6′	June 25, 1987	1952	clear
Grapevine Mountains, California	37°8′	117°27′	July 30, 1987	1850	clear
Moffett Field, California	37°53′	122°38′	June 25, 1987	2041	clear
Rogers Dry Lake, California	35°50′	117°50′	August 31, 1988	1800	clear

5. Steps 2 to 4 are iterated with varying water vapor amounts and different linear functions. The regression analysis is automated by incorporating the calculations into a nonlinear least squares program [*Donaldson and Tryon*, 1983]. Typically, after five iterations, the amount of water vapor in the total path and the best linear function for the spectral background level can be obtained.

6. The water vapor amount obtained in step 5 is converted to the vertical column water vapor amount based on the observational geometry and on the assumed atmospheric model.

The column water vapor and equivalent liquid water thickness over a vegetated area can be retrieved with similar procedures by replacing $T(\lambda)$ with the product of atmospheric gaseous transmittance and the liquid water transmittance and allowing the amount of liquid water to vary in step 5.

An example of curve fitting of a spectrum over a nonvegetated area was shown in Figure 5. Figure 9 shows a similar curve fitting of a spectrum but over a vegetated area. The retrievals of water vapor values over an entire scene from 19,840 spectra took approximately 200 min on a Micro-Vax III computer.

5. RESULTS

In order to test the ability to derive column water vapor and equivalent liquid water thickness of vegetation from AVIRIS spectra with our spectral curve fitting technique, retrievals were made from AVIRIS data collected over four sites; the Cuprite mining district in southwest Nevada, the Northern Grapevine Mountains in California, Moffett Field near San Francisco Bay in California, and Rogers Dry Lake in California. Table 1 lists the AVIRIS flight times as well as the latitudes and longitudes of these sites. All the measurements were made near local noon time on clear days with visibilities greater than 20 km (G. Vane, private communication, 1988). Table 2 gives general information on the water vapor derivations, including spectral averages, the water vapor bands and atmospheric models used in the retrievals.

In order to increase the signal-to-noise ratios and speed up the retrievals, the spectral data of individual pixels are usually averaged spatially on a 4 by 4 pixel basis. The spatial averaging increases the signal-to-noise ratio by a factor of 4 and increases the GIFOV to 80 x 80 m. The unaveraged spectra near 1 μm typically have signal-to-noise ratios of 50. Retrievals over the first three sites are made by curve fitting of the 1.14-μm water vapor band in the averaged spectra, and retrievals over Rogers Dry Lake are made by curve fitting both the 1.14-μm and the 0.94-μm water vapor bands in both averaged and original spectra. During the 1987 AVIRIS measurements over Cuprite, the Northern Grapevine Mountains, and Moffett Field there were no simultaneous measurements of atmospheric temperature, pressure and water vapor volume mixing ratio profiles. Column atmospheric water vapor amounts over these sites were retrieved with the "mid-latitude summer" atmospheric model in LOWTRAN 6 [*Kneizys et al.*, 1983]. During the 1988 AVIRIS measurement over the Rogers Dry Lake, radiosonde measurements of atmospheric temperature, pressure and water vapor volume mixing ratio (VMR) profiles were available. Column atmospheric water vapor amounts from the Rogers Dry Lake spectra were retrieved with the atmospheric profiles of the radiosonde measurements and also with the "mid-latitude summer" model of LOWTRAN 6.

The characteristics and the retrieval results for each site are described below.

TABLE 2. The General Information on Retrievals of Column Water Vapor Amounts From Five Sets of AVIRIS Spectral Data

Site	Pixel Averages	Water Vapor Band(s), μm	Atmospheric Model(s)
Cuprite, Nevada	4 by 4	1.14	mid-latitude summer model*
Grapevine Mountains, California	4 by 4	1.14	mid-latitude summer model*
Moffett Field, California	4 by 4	1.14	mid-latitude summer model*
Rogers Dry Lake, California (August 31, 1988)	4 by 4 and 1 by 1	1.14 and 0.94	Rawinsonde profiles and mid-latitude summer model*

*From *Kneizys et al.* [1983].

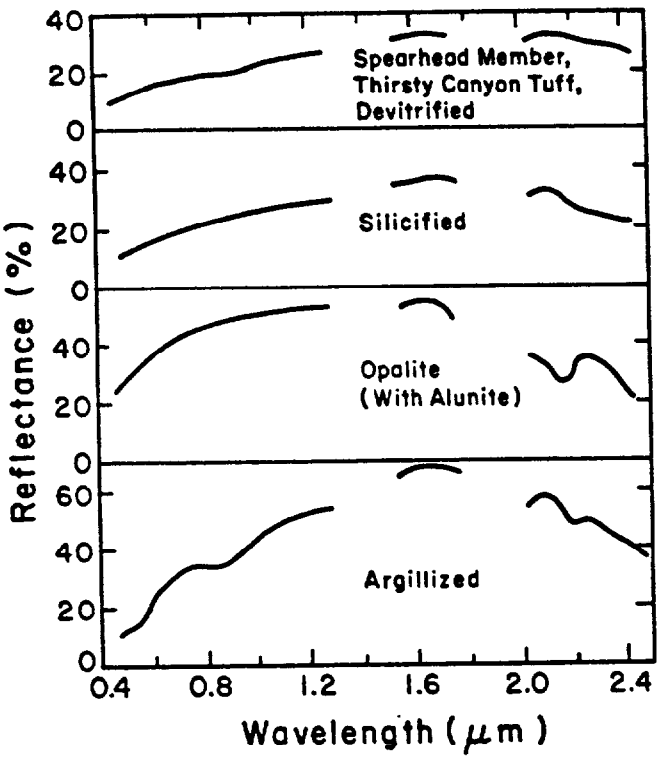

Fig. 10. Representative spectral reflectance curves of altered and unaltered rocks at Cuprite mining district in Nevada [from *Abrams et al.*, 1977].

5.1. *Cuprite, Nevada*

The Cuprite mining district includes exposures of rocks and soils with greatly different reflectances [*Abrams et al.*, 1977]. The reflectances within the AVIRIS scene vary by more than a factor of 3. Figure 10 shows examples of spectral reflectance curves of different rock types at the site. Figure 11*a* shows an image of the site. This image was processed from the radiance values of one spectral band centered at 1.037 μm in the atmospheric window. The bright regions represent areas with high reflectances, the maximum being approximately 0.65. The dark regions represent areas with low reflectances, the minimum being approximately 0.17. The scene contains a bright playa deposit (upper right corner) and nearby dark alluvial fans. Within the scene, there is less than 5% surface vegetation cover. More than 85% of the areas within the scene have less than 150 m of relief. There are no sources of water vapor, such as standing water, within the scene or in the nearby areas. Therefore it was assumed that the water vapor distribution within the scene was horizontally homogeneous. The main purpose for choosing the Cuprite site was to test the ability to derive column water vapor from surfaces with very different reflectances.

Column water vapor values were retrieved from the averaged spectra. Curve 1 of Figure 12 shows the statistical distribution of the column water vapor values over the entire scene. The mean of all the values is 0.97 cm, and the standard deviation 4.8%. This standard deviation demonstrates the high precision with which column water vapor values can be retrieved from the AVIRIS spectra in spite of significant variation in surface reflectance.

An image, processed from column water vapor values over the site, is shown in Figure 11*b*. In the vicinities of major reflectance contrast, the derived column water vapor values remain approximately the same. For example, the differences in column water vapor values between the

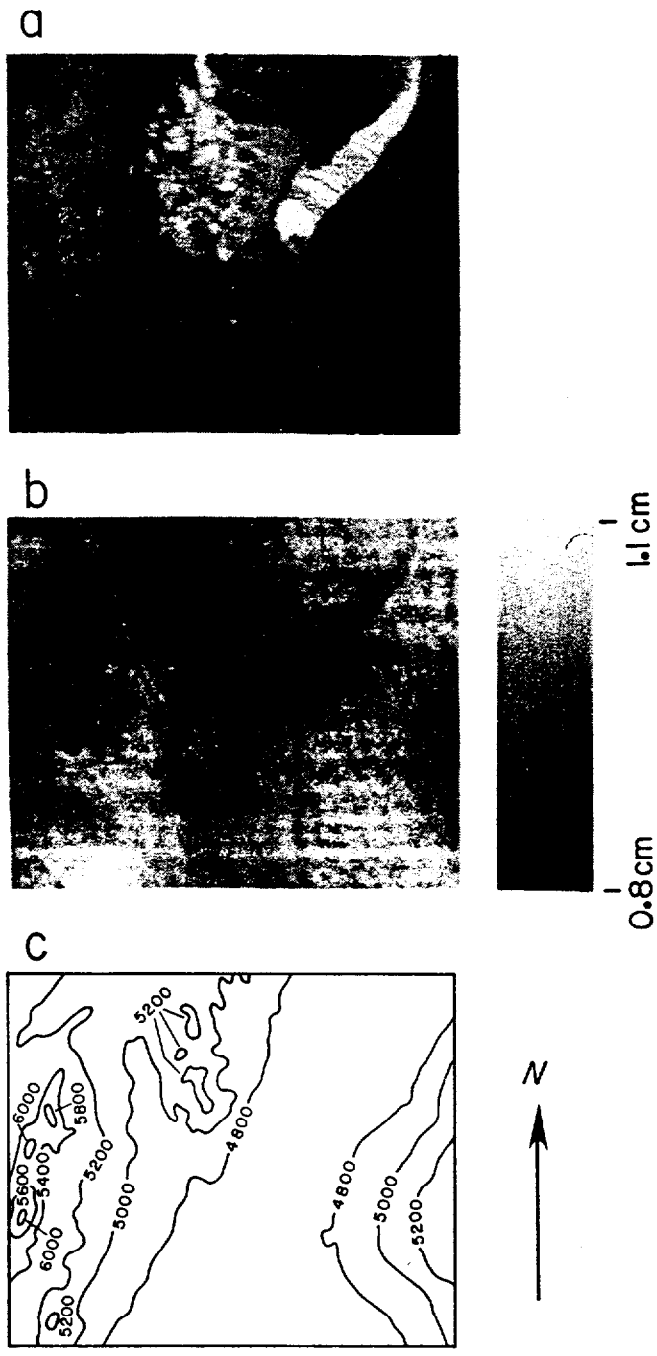

Fig. 11. Column water vapor retrievals from AVIRIS data measured over Cuprite, Nevada, on June 25, 1987. (*a*) An image of the scene processed from radiances of one channel centered at 1.037 μm, (*b*) a column water vapor image over the scene retrieved by curve fitting the 1.14-μm water vapor band absorption region, and (*c*) a topographic map of the scene. The elevations in the topographic maps are in units of feet (1 foot = 30.48 cm). The distance from left to right side of each of the images in this figure and in all subsequent figures is approximately 12 km.

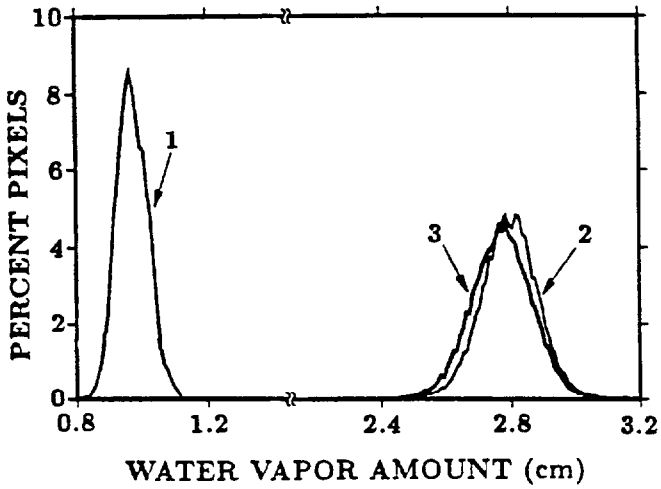

Fig. 12. Statistical distributions of column water vapor amounts over Cuprite site and over Rogers Dry Lake site. Curve 1 corresponds to Figure 11*b* with a mean of 0.971 cm and a standard deviation of 4.80%; curve 2 to Figure 16*b* with a mean of 2.797 cm and a standard deviation of 3.06%; and curve 3 to Figure 16*c* with a mean of 2.774 cm and a standard deviation of 3.30%.

highly reflecting playa (the upper right part of Figure 11*a*) and the nearby low reflectance alluvial fan region are less than 5%. This demonstrates that the derived column water vapor values are relatively insensitive to the absolute surface reflectance values.

Based on the discussion of scattering in section 4.7, it is expected that the single scattering will cause water vapor values retrieved over low reflectance areas to be smaller than those over high reflectance areas. However, the derived column water vapor values over the low reflectance alluvial fan areas are larger than those over the high reflectance playa areas. Therefore the small differences in retrieved water vapor amounts are attributed to the errors in the assumption of linear surface reflectances rather than to the single scattering effect.

A topographic map of the scene is shown in Figure 11*c*. The small variations in column water vapor values over the scene appear to be correlated with the surface topography rather than the surface reflectance differences.

5.2. *Northern Grapevine Mountains, California*

Figure 13 shows an AVIRIS image (1.037 μm), the water vapor image, and the topographic map for the scene over the Northern Grapevine Mountains in California. Elevation increases approximately 1000 m from left to right. The column water vapor values generally decrease from left to right as expected. The decrease of water vapor with increasing ground elevation can also be seen in Figure 14, which shows examples of normalized AVIRIS spectra over low, medium and high elevation areas. The peak absorption of the spectrum in the low elevation area is significantly larger than that of the spectrum in the high elevation area.

5.3. *Moffett Field, California*

Figure 15*a* shows a 0.86-μm image of Moffett Field near San Francisco Bay. The image shows the airport and part of San Francisco Bay. The regions covered by vegetation are bright because of its high reflectance at this wavelength. Spectra of the airport runway and San Francisco Bay were used to study the relative importance of path scattered radiation and direct reflected radiation, as described earlier.

Figure 15*b* shows examples of locations and amounts of column water vapor derived. The column water vapor amounts derived from spectra over vegetated areas are approximately equal to those derived from vegetation-free areas. The retrieved equivalent liquid water thicknesses of vegetation over different vegetated areas within the scene of Figure 15*a* range from 0.05 to 0.6 cm. Here discrete values are presented for clarity.

The derived column water vapor values over water areas vary significantly (see upper right of Figure 15*b*) because of the lower signal to noise ratios of the measured spectra. Our simple atmospheric transmission model is not sufficient for deriving column water vapor over water areas, since accurate derivation of column water vapor from water areas requires proper modeling of the single and multiple scattering processes.

5.4. *Rogers Dry Lake, California*

Figure 16*a* shows a 1.02-μm image of the Rogers Dry Lake scene. The variation of surface elevation over the entire scene is less than 50 m.

Figure 16*b* shows an image of column water vapor values derived by curve fitting the 0.94-μm band absorption feature in the 4 by 4 pixel averaged data and by using the atmospheric temperature, pressure and water vapor VMR profiles measured from a radiosonde that was released approximately 1 hour prior to the AVIRIS overflight. The statistical distribution of the column water vapor values is given in curve 2 of Figure 12. The mean of the water vapor values is 2.80 cm with a standard deviation of 3.06%. Retrievals from the 1.14-μm water vapor band are shown in Figure 16*c* and curve 3 of Figure 12. The mean of the column water vapor values from the 1.14-μm band is 2.77 cm, which is only 0.83% smaller than the mean of the water vapor values from the 0.94-μm band, and the corresponding standard deviation is 3.30%. The standard deviations, determined by finite signal-to-noise ratios of the measured spectra and by the deviations from linear in surface reflectances near 1 μm of different targets within the scene, demonstrate again the high precision with which column water vapor amounts can be derived from AVIRIS spectra. By comparing Figure 16*b* and Figure 16*c* with Figure 16*a*, it can be seen that the derived column water vapor values are independent of the absolute surface reflectances. The independence can be attributed to the offsetting effect on water vapor features between single scattered radiation and multiple scattered radiation, as discussed in section 4.7.

The mean column water vapor values of 2.80 and 2.77 cm agree remarkably well with the 2.8 cm of integrated column water vapor from the radiosonde measurement. The good agreement may be fortuitous since scattering is not explicitly modeled in our calculations and calculated transmittances with the Malkmus-band model are slightly dependent on the widths of the model parameters (J. Kiehl, private communication, 1988). Nevertheless, it is encouraging.

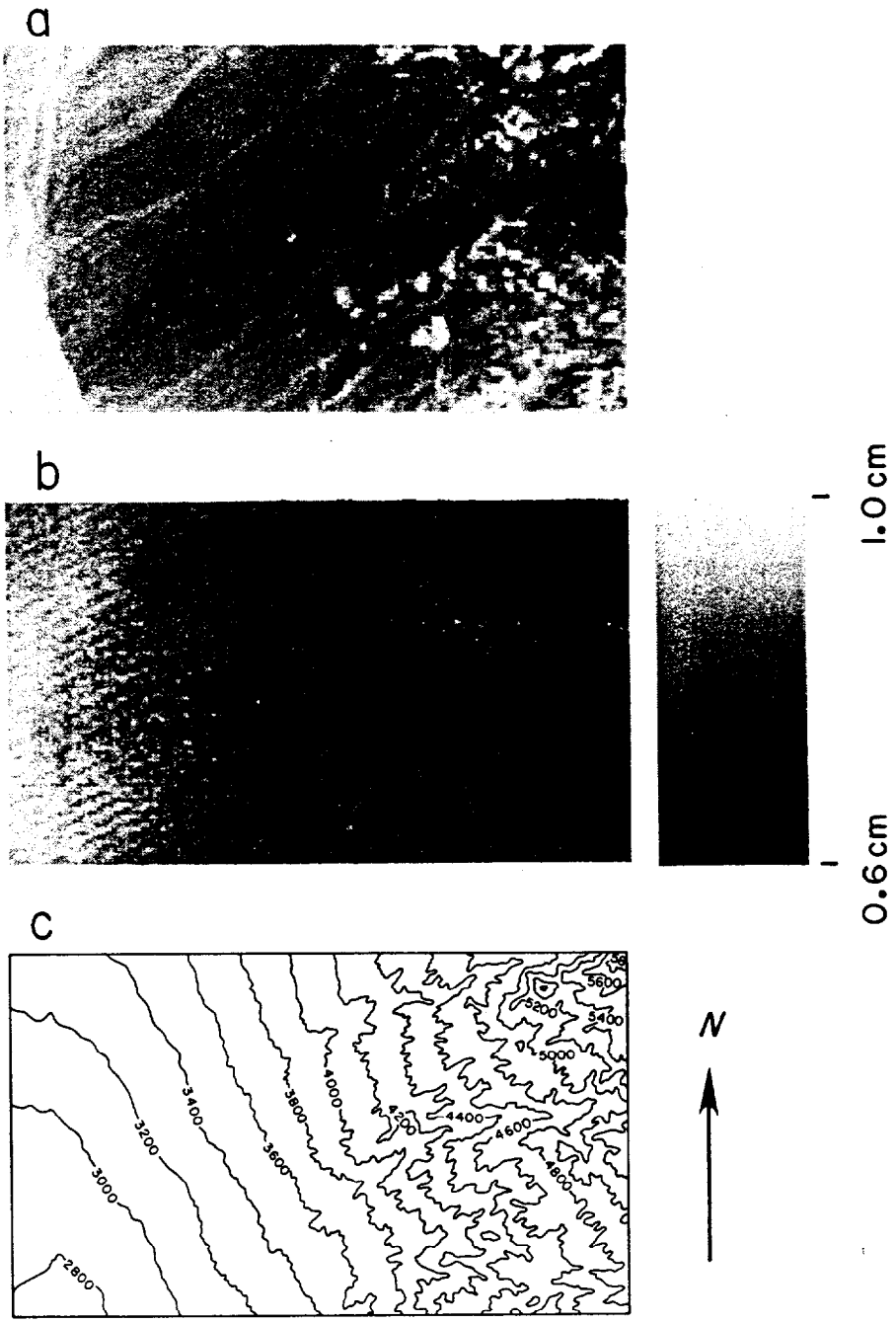

Fig. 13. Column water vapor retrievals from AVIRIS data measured over Grapevine Mountains in California on July 30, 1987. (*a*) An image of the scene processed from radiances of one channel centered at 1.037 μm, (*b*) a column water vapor image over the scene retrieved by curve fitting the 1.14-μm water vapor band absorption region, and (*c*) a topographic map of the scene. The elevations in the topographic map are in units of feet (1 foot = 30.48 cm).

Retrievals of column water vapor values from averaged spectra were also made by using the mid-latitude summer model from LOWTRAN 6 [*Kneizys et al.*, 1983]. The bottom layer temperature, pressure and water vapor VMR were linearly scaled to values at an elevation of 0.8 km for curve fitting both the 0.94- and the 1.14-μm absorption features. The shapes of both the temperature and the water vapor VMR profiles of the model, which were based on numerous measurements and also on theoretical calculations, are quite different from those measured with the single radiosonde released prior to the AVIRIS flight. The mean difference in column water vapor values derived with the mid-latitude summer model and those with the atmospheric model obtained from radiosonde measurement is 1.1%. The small difference indicates that the column water vapor retrievals are relatively insensitive to the assumed atmospheric models.

Column water vapor values were derived from the original AVIRIS spectra by curve fitting of the 1.14-μm water vapor band with the atmospheric model obtained

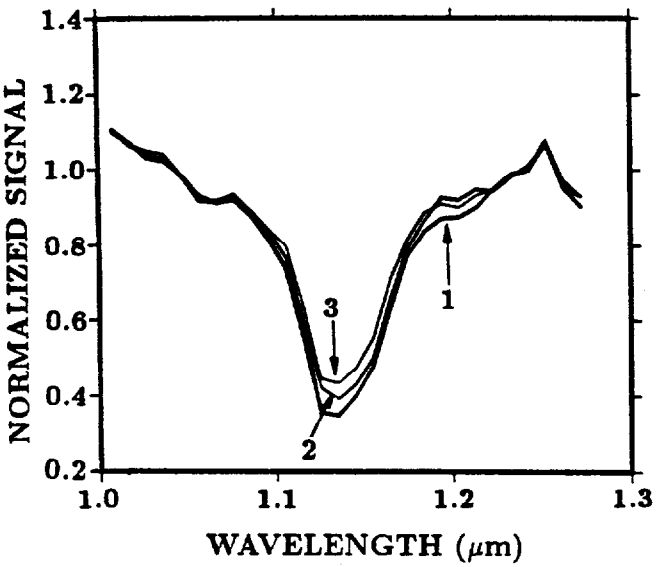

Fig. 14. Examples of spectra measured over elevations of approximately 0.9 km (curve 1), 1.2 km (curve 2) and 1.6 km (curve 3) in the Grapevine Mountains in California. The spectra have been normalized near 1.04 μm.

from the radiosonde. The mean of the column water vapor values is the same as that derived from the averaged data. However, the standard deviation increased to 8.9%. The increase in standard deviation is due to the lower signal-to-noise ratio of the original spectra.

6. MODEL SENSITIVITIES

The precision of the retrieved column water vapor amounts described above are controlled by the finite signal-to-noise ratio of the AVIRIS spectra and by the errors in the assumption of linear surface reflectances with wavelength in the water vapor band absorption regions. In addition to these, the accuracy of column water retrievals are affected by other factors, including errors in assumed atmospheric temperature, pressure and water vapor volume mixing ratio profiles, horizontal inhomogeneity in water vapor distributions (see section 7), and knowledge of the surface elevation at a GIFOV of 20 m.

6.1. *Temperature, Pressure and Water Vapor VMR Profiles*

Water vapor retrievals from AVIRIS data were also made with atmospheric models other than the mid-latitude *T*, *P*, and water vapor VMR profiles. Figure 17 shows four H_2O VMR profiles and the corresponding four temperature profiles used in testing retrievals. The temperatures and VMRs above 12 km were slightly modified from the original standard atmospheric models to simplify calculations. The modifications will not affect our conclusions because most of contributions to the 0.94- and 1.14-μm water vapor band absorptions are from the water vapor molecules in the lower part of the troposphere. Table 3 lists the retrieved column water vapor amounts from six of the AVIRIS spectra over Moffett Field for different atmospheric models. Taking the mid-latitude summer model as the standard, the deviations of column water vapor amounts retrieved with the other models are less than 7%. The mid-latitude winter model, which gives the largest deviation, is the least likely choice in actual retrievals of water vapor values from the spectra measured in the summer over mid-latitude regions. With reasonable choices of atmospheric models, it is expected that errors in estimated water vapor amounts due to atmospheric model assumptions will be 5% or less. Therefore the derived column water vapor amount is relatively insensitive to the assumed atmospheric models.

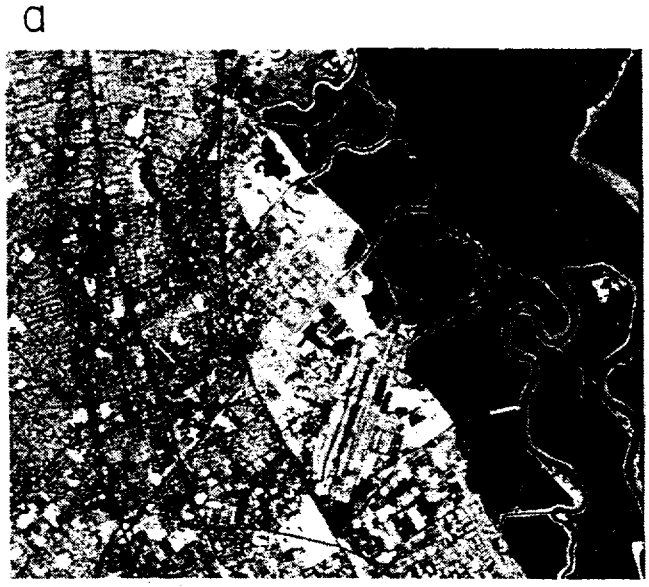

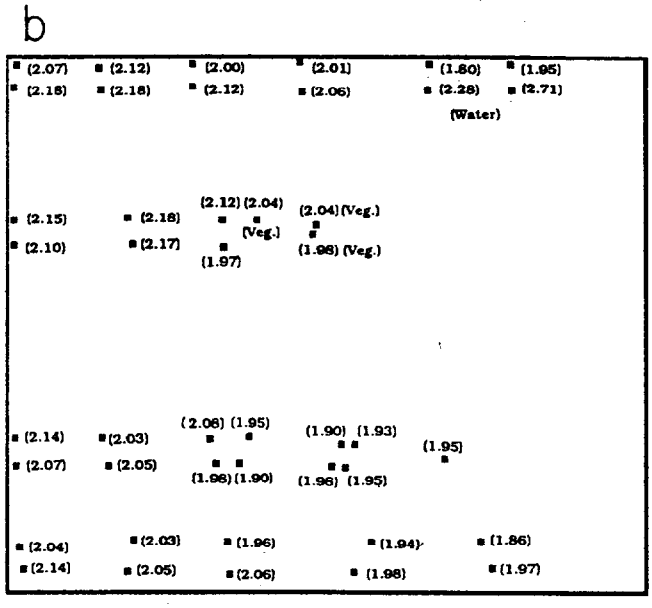

Fig. 15. Column water vapor retrievals from AVIRIS data measured over Moffett Field near San Francisco Bay in California on July 30, 1987. (*a*) An image of the scene processed from radiances of one channel centered at 0.86 μm. The airport and part of San Francisco Bay can be seen in the image. The brightest regions in the image are areas with vegetation because the reflectance of vegetation at 0.88 μm is greater than most other surface targets. (*b*) Spatial locations at which column water vapor was retrieved and the derived column water vapor values (in units of centimeters) at the locations.

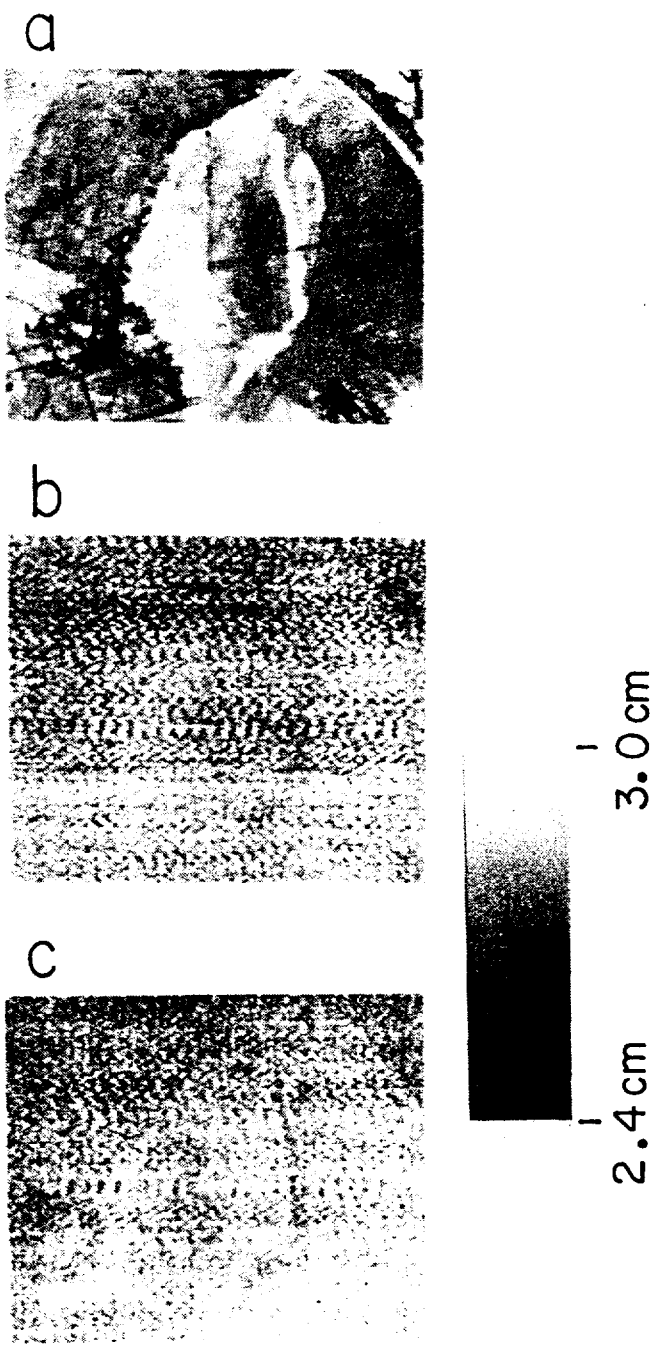

Fig. 16. Column water vapor retrievals from AVIRIS data measured over Rogers Dry Lake in California on August 31, 1988. (*a*) An image of the scene processed from radiances of one channel centered at 1.02 μm, (*b*) a column water vapor image over the scene retrieved by curve fitting the 0.94-μm water vapor band absorption region, and (*c*) same as in Figure 16*b*, except retrieved from the 1.14-μm water vapor band.

6.2. *Boundary Layer Inversion*

If an inversion is present during data acquisition and normal atmospheric models are used in the column water vapor amount retrievals from AVIRIS spectra, systematic errors may be introduced in the derived column water vapor amounts. We have retrieved column water vapor amounts from six of the AVIRIS spectra over Moffett Field by assuming (1) the normal mid-latitude summer model, (2) the same model except that the water vapor VMRs are inverted between 0 and 2 km, and (3) the same model except that both the temperatures and the water vapor VMRs are inverted between 0 and 2 km in the retrievals. The results show that the inversions introduce errors of less than 3%. Therefore the derived column water vapor amount is also relatively insensitive to boundary layer inversion effects.

6.3. *Surface Elevation*

Atmospheric pressure decreases monotonically with altitude. Because of the pressure dependence of Lorentz lines, accurate derivation of column water vapor amounts from AVIRIS spectra requires the knowledge of surface pressures, or elevations. In order to test the sensitivity of column water vapor retrievals to surface elevation, retrievals were made from the same set of AVIRIS spectra

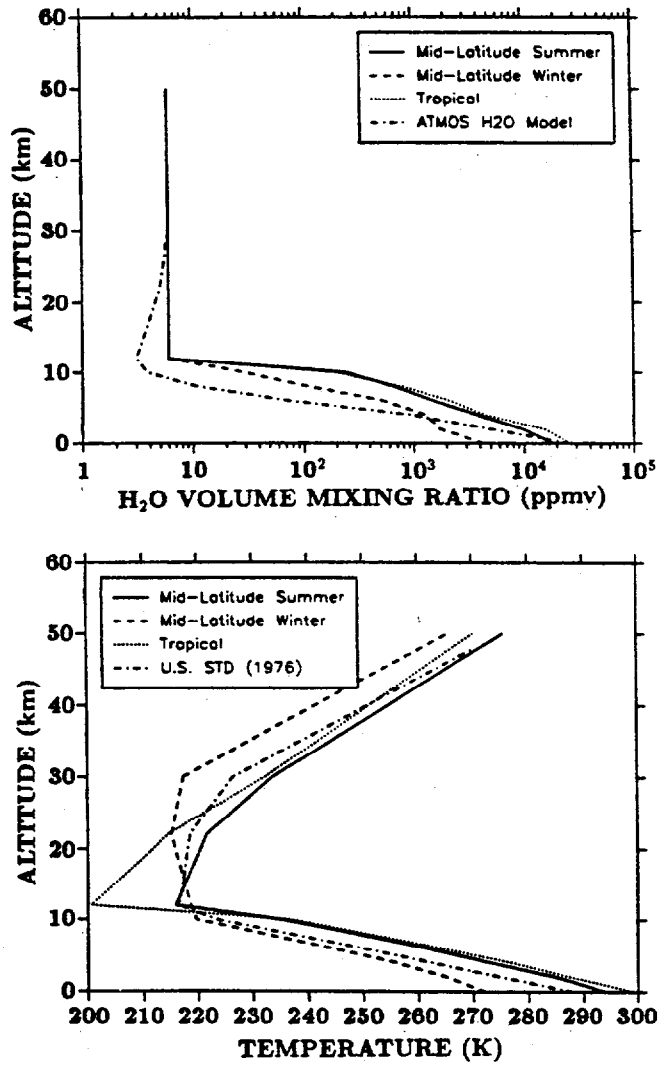

Fig. 17. (Top) Four water vapor volume mixing ratio profiles and (bottom) four temperature profiles used in the study of the sensitivities of column water vapor retrievals on atmospheric profiles.

TABLE 3. Averaged Column Water Vapor Amounts Retrieved With Different Atmospheric Models From Six AVIRIS Spectra Measured Over the Moffett Field Airport Runway

	Mid-Latitude Summer Model*	Tropical Model*	ATMOS Model†	Mid-Latitude Winter Model*
Averaged water vapor, cm	1.984	1.956	1.901	2.110
Deviation from mid-latitude summer model	0.00%	-1.41%	-4.18%	6.35%

*From *Kneizys et al.* [1983].

†From R.H. Horton (private communication, 1986). ATMOS stands for the Atmospheric Trace Molecule Spectroscopy experiment.

by using the mid-latitude summer model with (1) all the layers above 0 km, and (2) only layers above 0.5, 1.0, 1.5 and 2.0 km. The results indicate that a 0.5-km error in the assumed surface elevation introduces an error of approximately 5% in the derived column water vapor amounts. Therefore knowledge of surface elevations at a GIFOV of 20 m and with accuracy better than 300 m will be necessary when deriving column water vapor from AVIRIS/HIRIS spectra with an accuracy of 3%.

7. SUMMARY AND CONCLUSIONS

We have developed a method for the quantitative derivation, at high spatial resolution, of column atmospheric water vapor amounts from imaging spectrometer measurements of reflected solar radiation on clear days with visibilities of 20 km or greater. The precision of the derived column water vapor amounts from sets of AVIRIS data is approximately 5%. The retrieved column water vapor amounts are independent of the surface reflectance. Therefore the absolute surface reflectances and radiance values are not required for column water vapor retrievals when the concentrations of atmospheric aerosols are low.

Because path scattered radiation is not explicitly modeled, our method is not directly applicable to situations when the atmospheric aerosol concentrations are high, particularly when large amounts of stratospheric aerosols are present. A thorough treatment of multiple scattering effects is needed when aerosol concentrations are high.

The column water vapor values derived from the set of AVIRIS spectral data over Rogers Dry Lake in California agree very well with the radiosonde measurement. However, in order to assess the accuracy of column water vapor derivations on clear days with our technique, more AVIRIS spectral data with nearly simultaneous measurements of water vapor profiles with radiosondes are necessary. These data will be available in the near future.

Simultaneous retrievals of column atmospheric water vapor amounts and the equivalent liquid water thicknesses of surface vegetation have also been made. The derived equivalent liquid water thicknesses is related to the number of liquid water molecules that interacted with the incident solar radiation, and therefore related to the moisture content of vegetation. However, the exact relationship between EWT and the true vegetation canopy water content has not yet been established.

Preliminary error analysis shows that the derived column water vapor from AVIRIS spectra is relatively insensitive to the assumed atmospheric models, and to the inversions of temperature and water vapor VMRs in the boundary layer between about 0 and 2 km. The analysis also shows that accurate retrievals of water vapor values require the knowledge of surface elevations (or pressures) to better than about 300 m (or 96%). A more complete error and sensitivity analysis could be made by analyzing spectra from a greater range of column water vapor values.

Because the observational angle and the solar zenith angle are not zero, there are contributions to the absorptions from water vapor molecules from regions outside the pixel observed. Consequently, a spatial smearing effect is present in our derived column water vapor values. The magnitude of the spatial smearing is estimated to be 500 m or greater and depends on the three-dimensional water vapor distribution and on the solar and observational geometry. If the water vapor distribution over a few-kilometer range is nearly uniform horizontally, the smearing effect is irrelevant.

Initially, attempts were made to use LOWTRAN 6 [*Kneizys et al.*, 1983] to calculate atmospheric transmission spectra. However, LOWTRAN 6 significantly underestimates the absorption in the edges of the 1.14- and 0.94-μm water vapor bands. This problem has been corrected in the recently released LOWTRAN 7 [*Kneizys et al.*, 1988].

Since the measured spectra over bodies of water also contain the atmospheric water vapor absorption features (see Figure 8*a*), it might be possible to derive column atmospheric water vapor from these spectra if proper modeling of multiple scattering and surface specular reflection can be made. In the case of snow, the relative shifts of absorption bands of water vapor, liquid water and ice (see Figure 6) should allow the simultaneous retrievals of column atmospheric water vapor, liquid content of snow near the surface, and the snow grain size distributions from image spectra.

Based on the results from AVIRIS, the technique described is directly applicable to HIRIS, which is slated to acquire data world wide on a target of opportunity basis from the Polar Orbiting Platform beginning in 1997.

Acknowledgments. The authors are grateful to J. Conel and R. O. Green of the Jet Propulsion Laboratory for providing the AVIRIS spectral data and radiosonde data, to B. P. Briegleb and J. T. Kiehl of the National Center for Atmospheric Research for providing narrow-band model parameters, to F. X. Kneizys and L. W. Abreu of the Air Force Geophysics Laboratory for providing an early copy of

LOWTRAN7 program, and to J. Boardman of CSES/CIRES, University of Colorado for discussions on spatial smearing. This work was partly supported by the Cooperative Institute for Research in Environmental Sciences of the University of Colorado at Boulder through a Visiting Fellowship and by the Jet Propulsion Laboratory, California Institute of Technology under contract 958039.

REFERENCES

Abrams, M. J., R. P. Ashley, L. C. Rowan, A. F. H. Goetz, and A. B. Kahle, Mapping of hydrothermal alteration in the Cuprite mining district, Nevada, using aircraft scanner images for the spectral region 0.46 to 2.36 μm, *Geology, 5*, 713–718, 1977.

Allen, W. A., H. W. Gaussman, A. J. Richard-son, and J. P. Thomas, Interaction of isotropic light with a compact plant leaf, *J. Opt. Soc. Am., 59*, 1376–1379, 1969.

Allen, W. A., H. W. Gausman, A. J. Richardson, and R. Cardenas, Water and air changes in grapefruit, corn, and cotton leaves with maturation, *Agron. J., 63*, 393–394, 1971.

Bowker, D. E., R. E. Davis, D. L. Myrick, K. Stacy, and W. T. Jones, Spectral reflectances of natural targets for use in remote sensing studies, *NASA Ref. Publ. 1139*, 1985.

Bunting, J. T., and R. P. d'Entremont, Improved cloud detection utilizing defense meteorological satellite program near infrared measurements, *AFGL-TR-82-0027*, pp. 10–11, Air Force Geophys. Lab., Bedford, Mass., 1982.

Butler, D. M., et al., From pattern to process: The strategy of the Earth Observing System, in *NASA Earth Observing System*, vol. II, pp. 1–29, NASA, Washington D.C., 1987.

Camillo, P., A canopy reflectance model based on an analytical solution to the multiple scattering equation, *Remote Sens. Environ., 23*, 453–477, 1987.

Condit, H. R., The spectral reflectance of American soils, *Photogramm. Eng., 36*, 955–965, 1970.

Dickinson, R. E., Land surface processes and climate-surface albedos and energy balance, *Adv. Geophys., 25*, 305–353, 1983.

Dickinson, R. E., P. J. Sellers, and D. S. Kimes, Albedos of homogeneous semi-infinite canopies: Comparison of two-stream analytic and numerical solutions, *J. Geophys. Res., 92*, 4282–4286, 1987.

Donaldson, J. R., and P. V. Tryon, Nonlinear least squares regression using STARPAC, *NBS Tech. Note 1068*, pp. 1–46, Nat. Bur. of Stand., Gaithersburg, Md., 1983.

Esaias, W., et al., Moderate resolution imaging spectrometer, in *Earth Observing System*, vol. IIb, *Instrument Panel Report*, pp. 49-53, NASA, Washington, D.C., 1986.

Farmer, C. B., G. C. Toon, P. W. Schaper, J.-F. Blavier, and L. L. Lowes, Stratospheric trace gases in the spring 1986 Antarctic atmosphere, *Nature, 329*, 126–130, 1987.

Goetz, A. F. H., G. Vane, J. Solomon, and B. N. Rock, Imaging spectrometry for Earth remote sensing, *Science, 228*, 1147–1153, 1985.

Goetz, A. F. H., et al., High resolution imaging spectrometer: Science opportunities for the 1990s, in *Earth Observing System*, vol. IIC, *Instrument Panel Report*, pp. 1–65, NASA, Washington, D.C., 1987.

Goetz, A. F. H., and M. Herring, The high resolution imaging spectrometer (HIRIS) for Eos, *IEEE Trans. Geosci. Remote Sens., 27*, 136–144, 1989.

Goldman, A., F. G. Fernald, F. J. Murcray, F. H. Murcray, and D. G. Murcray, Spectral least squares quantification of several atmospheric gases from high resolution infrared solar spectra obtained at the south pole, *J. Quant. Spectrosc. Radiat. Transfer, 29*, 189–204, 1983.

Goody, R. M., A statistical model for water vapor absorption, *Q. J. R. Meteorol. Soc., 78*, 165–169, 1952.

Gordon, H. R., and A. Y. Morel, *Remote Assessment of Ocean Color for Interpretation of Satellite Visible Imagery: A Review*, pp. 114–120, Springer–Verlag, New York, 1983.

Grant, L., Diffuse and specular characteristics of leaf reflectance, *Remote Sens. Environ., 22*, 309–322, 1987.

Hogg, D. C., F. O. Guiraud, J. B. Snider, M. T. Decker, and E. R. Westwater, A steerable dual-channel microwave radiometer for measurement of water vapor and liquid in the troposphere, *J. Appl. Meteorol., 22*, 789–806, 1983.

Hunt, G. R., and R. P. Ashley, Spectra of altered rocks in the visible and near infrared, *Econ. Geol., 74*, 1613–1629, 1979.

Iqbal, M., *An Introduction to Solar Radiation*, pp. 43–95, Academic, San Diego, Calif., 1983.

Justice, C. G., and M. V. Paris, A model for solar spectral irradiance and radiance at the bottom and top of a cloudless atmosphere, *J. Clim. Appl. Meteorol., 24*, 193–205, 1984.

Kirk, J. T. O., Solar heating of water bodies as influenced by their inherent optical properties, *J. Geophys. Res, 93*, 10897–10908, 1988.

Kneizys, F. X., E. P. Shettle, W. O. Gallery, J. H. Chetwynd, L. W. Abreu, J. E. A. Selby, S. A. Clough, and R. W. Fenn, Atmospheric transmittance/radiance: Computer code LOWTRAN 6, *AFGL–TR–83–0187*, Air Force Geophys. Lab., Bedford, Mass., 1983.

Kneizys, F. X., E. P. Shettle, L. W. Abreu, J. H. Chetwynd, G. P. Anderson, W. O. Gallery, J. E. A. Selby, and S. A. Clough, Users guide to LOWTRAN 7, *AFGL–TR–8–0177*, Air Force Geophys. Lab., Bedford, Mass., 1988.

Knipling, E. B., Physical and physiological basis for the reflectance of visible and near-infrared radiation from vegetation, *Remote Sens. Environ., 1*, 155–159, 1970.

Malkmus, W., Random Lorentz band model with exponential-tailed S line intensity distribution function, *J. Opt. Soc. Am., 57*, 323–329, 1967.

Mankin, W. G., Fourier transform method for calculating the transmittance of inhomogeneous atmosphere, *Appl. Opt., 18*, 3426–3433, 1979.

Otterman, J., Albedo of a forest modeled as a plane with dense protrusions, *J. Clim. Appl. Meteorol., 23*, 297–307, 1984.

Palmer, K. F., and D. Williams, Optical properties of water in the near infrared, *J. Opt. Soc. Am., 64*, 1107–1110, 1974.

Prabhakara, C., H. D. Chang, and A. T. C. Chang, Remote sensing of precipitable water over the oceans from Nimbus 7 microwave measurements, *J. Appl. Meteorol., 31*, 59–68, 1982.

Reuter, D., J. Susskind, and A. Pursch, First-guess dependence of a physically based set of temperature-humidity retrievals from HIRS2/MSU data, *J. Atmos. Oceanic Technol., 70–83*, 1988.

Rinsland, C. P., A. Goldman, and G. M. Stokes, Identification of atmospheric C_2H_2 lines in the 3230-3340 cm^{-1} region of high resolution solar absorption spectra at the National Solar Observatory, *Appl. Opt., 24*, 2044–2066, 1985.

Rodgers, C. D., and C. D. Walshaw, The computation of infra-red cooling rate in planetary atmosphere, *Q. J. R. Meteorol. Soc., 92*, 67–92, 1966.

Rothman, L. S., R. R. Gamache, A. Goldman, L. R. Brown, R. A. Toth, H. M. Pickett, R. L. Poynter, J.-M. Flaud, C. Camy-peyret, A. Barbe, N. Husson, C. P. Rinsland, and

M. A. H. Smith, The HITRAN database: 1986 edition, *Appl. Opt., 26,* 4058–4097, 1987.

Russell, J. M., III, C. B. Farmer, C. P. Rinsland, R. Zander, L. Froidevaux, G. C. Toon, B. C. Gao, and J. H. Shaw, Measurements of odd nitrogen in the stratosphere by the ATMOS experiment on Spacelab 3, *J. Geophys. Res., 93,* 1718–1736, 1988.

Shaw, J. H., N. Tu, and S. L. Agresta, Sources of systematic errors in the line intensities, *Appl. Opt., 24,* 2437–2441, 1985.

Stoner, E. R., and M. F. Baumgardner, Physiochemical, site and bidirectional reflectance factor characteristics of uniformly moist soils, pp. 1–50, *NASA CR-160571,* 1980.

Susskind, J., J. Rosenfield, and D. Reuter, Remote sensing of weather and climate parameters from HIRS2/MSU on TIROS-N, *J. Geophys. Res., 89,* 4677–4697, 1984.

Tucker, C. J., Remote sensing of leaf water content in the near infrared, *Remote Sens. Environ., 10,* 23–32, 1980.

Vane, G. (Ed.), Airborne visible/infrared imaging spectrometer (AVIRIS), JPL Publ. 87–38, Jet Propul. Lab., Pasadena, Calif., 1987.

Verstraete, M. M., Radiation transfer in plant canopies: Scattering of solar radiation and canopy reflectance, *J. Geophys. Res., 93,* 9483–9494, 1988.

Volz, F. E., Economical multispectral sun photometer for measurements of aerosol extinction from 0.44 μm to 1.6 μm and precipitable water, *Appl. Opt., 13,* 1732–1733, 1974.

Warren, S. G., Optical constants of ice from the ultraviolet to the microwave, *Appl. Opt., 23,* 1206–1223, 1984.

Wessman, C. A., J. D. Aber, D. L. Peterson, and J. M. Melillo, Remote sensing of canopy chemistry and nitrogen cycling in temperate forest ecosystems, *Nature, 335,* 154–156, 1988.

B.-C. Gao and A. F. H. Goetz, Center for the Study of Earth from Space, Cooperative Institute for Research in Environmental Sciences, Campus Box 449, University of Colorado, Boulder, CO 80309.

(Received May 22, 1989;
revised August 2, 1989;
accepted August 15, 1989.)